

Rearomatization of trifluoromethyl sulfonyl dihydropyridines: Thermolysis vs photolysis

Guadalupe Firpo¹ | María V. Cooke¹ | Walter J. Peláez¹  | Guillermo M. Chans² | Gustavo A. Argüello¹ | Elizabeth Gómez³ | Cecilio Alvarez-Toledano³

¹INFIQC, Departamento de Físicoquímica, Facultad de Ciencias Químicas, Universidad Nacional de Córdoba, Córdoba, Argentina

²Facultad de Ingeniería, Universidad Anáhuac (México Norte), Huixquilucan, Mexico

³Instituto de Química, Universidad Nacional Autónoma de México, México, DF, Mexico

Correspondence

W. J. Peláez, INFIQC, Departamento de Físicoquímica, Facultad de Ciencias Químicas, Universidad Nacional de Córdoba, Ciudad Universitaria, X5000HUA Córdoba, Argentina.
Email: waldemar31@fcq.unc.edu.ar

Funding information

MINCYT-CONACYT (2013-2016), Grant/Award Number: MX/12/07; SECyT-UNC; MINCYT; FONCyT; CONACYT 191400 FOINS; CONICET

Abstract

In this article, we describe the static gas-phase pyrolysis, microwave-induced pyrolysis, and photolysis reactions of trifluoromethyl sulfonyl dihydropyridines. The goal of this work was to find a methodology that allows obtaining of substituted pyridines—which are known to be difficult to synthesize—to be reused in a new substitution reaction. We demonstrated that it is possible to achieve the rearomatization process by the elimination of the trifluoromethyl sulfonyl moiety through the 3 processes, with the static pyrolysis being the best method to obtain the substituted pyridines. In addition, we propose the 1,4-elimination ($\text{CF}_3\text{SO}_2 + \text{H}$) as the first step, since it is the less energetic process, as has also been corroborated by calculations. A competitive reaction (CO_2 extrusion) also occurs, yielding undesired products.

KEYWORDS

gas-phase and microwave-induced pyrolysis, rearomatization reactions, TD-DFT calculations, trifluoromethyl sulfonyl dihydropyridines

1 | INTRODUCTION

As part of our ongoing project on sulfonyl derivatives as bioactive heterocyclic compounds, our research has been focused on exploring the consequences of a N-SO₂-R linkage on the stereoelectronic properties of some 1-benzenesulfonyl-1,2,3,4-tetrahydroquinolines (compounds **1-4**, Figure 1). Recently, we reported a detailed analysis of UV spectra and the molecular orbitals involved in electronic transitions and a conformational study of 1-benzenesulfonyl-1,2,3,4-tetrahydroquinoline derivatives conducted using the time-dependent density functional theory (TD-DFT) (B3LYP/6-31 + G(d,p)) method. Good correlations between theoretical and

experimental data for the energy transitions and molar extinction coefficients of the compounds studied have been obtained and were presented for the first time.^[1]

In addition, we recently reported the thermal behavior of some trifluoromethyl-1*H*,3*H*-pyrrolo[1,2-*c*]thiazole-2,2-dioxides (compounds **5-8**, Figure 1) evaluated by comparing flash vacuum pyrolysis (at 475°C) with the microwave-induced pyrolysis (MIP at 240°C). In both cases, the azafulvenium methide intermediate was involved and claimed to be responsible for the interesting compounds obtained.^[2,3]

Currently, we are interested in trifluoromethyl sulfonyl dihydropyridines and their benzene-fused derivatives (compounds **9** and **10**, Figure 1).

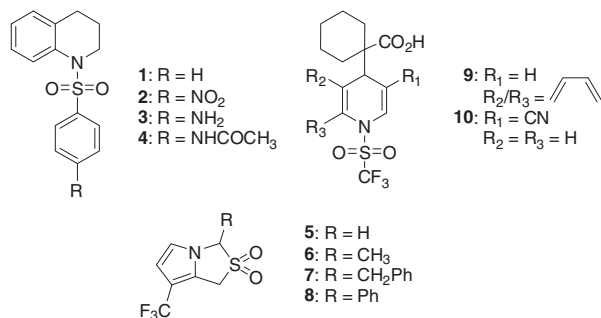


FIGURE 1 1-Benzenesulfonyl-1,2,3,4-tetrahydroquinolines (**1-4**) and 2,2-dioxo-pyrrolo-thiazole (**5-8**) previously studied, and trifluoromethyl sulfonyl dihydropyridines (**9** and **10**) studied in this work

Pyridines emerge as one of the most prevalent heterocyclic structural units in pharmaceutical and agrochemical targets, as well as in material science.^[4-6] Pyridine derivatives are widely known as gifted starting materials for the synthesis of dihydropyridines, tetrahydropyridines, and piperidines, which have been used as intermediates in alkaloid synthesis,^[7,8] in nicotinamide adenine dinucleotide hydrogen models,^[9,10] and as important biologically active structures.^[11-15] It is known that one key aspect about the reactivity of pyridine and its derivatives is that once activated, they can react with a large variety of nucleophiles to afford substituted dihydropyridines,^[7,16-23] which, after the elimination of the trifluoromethyl sulfonyl moiety, can further be reactivated to undergo secondary nucleophilic additions. Following this approach, the activation of aza-aromatic compounds can be achieved through the nitrogen atom by alkyl chloroformates,^[24-26] acid chlorides,^[27,28] or triflic anhydride,^[29-31] via their pyridinium salts.^[32] Taking advantage of the pyridine activation versatility, ours and other research groups have described the direct synthesis of functionalized polycyclic δ - and γ -lactones^[33-36] via a double nucleophilic addition of bis(trimethylsilyl)ketene acetals to previously activated pyridines. Recently, it has been shown that this reaction can be extended to other aza-aromatic substrates such as pyrazine, quinoxaline, and pyrimidine, where the course of the reaction depends on the activating agent.^[37,38] We also reported that this method could be applied to pyridine N oxide, affording tetrahydrofuro[3,2-*b*]pyridine-2(3*H*)-ones through a double-activation procedure and an unexpected decarboxylation step.^[36] Monoaddition (dihydropyridines) and double-addition products (tetrahydropyridine-fused lactones) are of interest because of their biological activities.^[16,17,39-42]

Specifically, we are interested in the reactivity of the monoactivated trifluoromethyl sulfonyl derivatives and

how the trifluoromethanesulfonyl moiety can be removed to afford the aromatic pyridine. The goal of the present work is to find a good methodology to complete the sequence of activation, nucleophilic reaction, and deprotection that will allow having an activated substrate again to perform new substitutions and thus opening endless synthetic possibilities. Therefore, a comparison of 3 methodologies (MIP, static gas-phase pyrolysis, and photolysis at 254 nm) aimed at the synthesis of the target compound is presented.

2 | RESULTS AND DISCUSSION

2.1 | UV characterization

The UV/visible characterization was performed in acetonitrile (ACN), methanol (MeOH), ethanol (EtOH), and water (only for compound **10**) with the main objective of knowing about the nature of the transitions (either $\pi \rightarrow \pi^*$ or $n \rightarrow \pi^*$) involved in the main absorption bands. The experimental absorption maxima were determined with the aid of the second derivative spectra.

Compound **9** presents 4 absorption bands in ACN: 2 intense broad bands at short wavelengths, 205 nm ($\epsilon = (22.0 \pm 0.4) \times 10^3 \text{M}^{-1} \text{cm}^{-1}$) and 226 nm (broad shoulder, $\epsilon = (11.4 \pm 0.2) \times 10^3 \text{M}^{-1} \text{cm}^{-1}$), and 2 bands of very small intensity at longer wavelengths, 269 nm ($\epsilon = (6.70 \pm 0.03) \times 10^2 \text{M}^{-1} \text{cm}^{-1}$) and 277 nm ($\epsilon = (5.4 \pm 0.02) \times 10^2 \text{M}^{-1} \text{cm}^{-1}$). No clear trend in the band shifting was observed when the spectra were taken in different solvents (EtOH, MeOH, see the spectra in page S3 of the Supporting Information). For that reason, the determination of the transition that occurs was performed through TD-DFT calculations (B3LYP/6-31 + G(d,p)) as it was reported in our previous work on 1-benzenesulfonyl-1,2,3,4-tetrahydroquinoline derivatives.^[1] After performing the optimization and analyzing the symmetry of the molecular orbitals involved in each transition, we established that all of them are of $\pi \rightarrow \pi^*$ nature.

On the other hand, compound **10** presents 2 well-defined absorption regions in ACN with maxima determined again by the second derivative methodology. The shorter wavelength band possesses a shoulder at 220 nm ($\epsilon = (7.8 \pm 0.3) \times 10^3 \text{M}^{-1} \text{cm}^{-1}$), whereas the other band appears centered at 270 nm ($\epsilon = (5.0 \pm 0.2) \times 10^3 \text{M}^{-1} \text{cm}^{-1}$). Changing the polarity of the solvents (EtOH, MeOH, and H₂O, see the spectra in page S5 in the Supporting Information) a bathochromic shifting is observed, allowing us to assess that all transitions are $\pi \rightarrow \pi^*$. The TD-DFT calculations (B3LYP/6-31 + G(d,p)) corroborate this assumption.

2.2 | Reactions of 1-(1-((trifluoromethyl)sulfonyl)-1,4-dihydroquinolin-4-yl)cyclohexane-1-carboxylic acid (**9**)

The identification of all products obtained from compound **9** under different reaction conditions was performed by a careful analysis of the data, obtained from gas chromatography (GC)/mass spectrometry (MS) and nuclear magnetic resonance (NMR) techniques. Under all reaction conditions, it was possible to obtain the desired aromatized ring (1-(quinolin-4-yl)cyclohexane-1-carboxylic acid, **11**) after the loss of the $\text{CF}_3\text{-SO}_2 + \text{H}$; nevertheless, other competitive processes occurred, which generated undesired compounds with variable yields depending on the reaction conditions (Table 1). Photolysis, in turn, was the most unfavorable method, affording low yields of **11** and almost 50% of an unidentified insoluble solid. Nevertheless, important mechanistic information was obtained from this experiment. For example, the detection of the product of $m/z = 345$ (4-cyclohexyl-1-((trifluoromethyl)sulfonyl)-1,4-dihydro-quinoline **14**) allows us to postulate that the loss of CO_2 is competing with the fragmentation of the N-S bond.

The analysis of the results obtained by MIP shows that this method is barely more efficient than photolysis in the production of the desired aromatized compound. In particular, the attempts to improve the yield of **11** were unsuccessful, since the change of 10°C in the reaction temperature raised the yield of by-products (the 3 isomers of (trifluoromethyl)sulfonyl-quinoline, **15a-c**) by as much as 45%, while **11** is only increased by less than 10%. The detection of compound **16** (1-((trifluoromethyl)sulfonyl)-1,4-dihydroquinoline, $m/z = 263$) supports the idea of a competitive reaction where the C-C bond breaks apart, either directly from **9** or from **14**, where the loss of CO_2 should have already occurred. Only through gas-phase pyrolysis did we find a reasonable balance between the target compound and the by-products. Attempts to study the gas-phase pyrolysis at temperatures lower than 200°C were ineffective. By increasing the exposure time, the yield of **11** was doubled; nevertheless, the undesired products also increased. It is worth mentioning that Fourier transform infrared (FT-IR) analysis of the gases produced during pyrolysis assessed the presence of HCF_3 and SO_2 , identified by comparison of pure samples.

By unraveling the by-products obtained, regardless of the method used, another interesting outcome is noticed. The formation of 3 isomers of **15** proves that the S-C bond is strong enough to allow the migration of the trifluoromethyl sulfonyl group ($-\text{SO}_2\text{CF}_3$) toward the aromatic ring, even though it should suffer its own fragmentation, as confirmed by the detection of HCF_3 and SO_2 through FT-IR measurements.

TABLE 1 Pyrolysis (microwave induced and gas phase) vs photolysis of compound **9**

Compound	Chemical Structure	m/z	Time, min	Reaction	Reaction condition	11	12	13	14	15a-c	16	17a-c
		364	11.7	Gas chromatography		1	17	0	2	14	0	5
		255	9.2	Photolysis	Acetonitrile (ACN), 254 nm	1	13	0	2	14	0	5
		211	6.6	Microwave pyrolysis	ACN, 230°C, 10 min	11	6	0	0	10	1	0
		209	6.3	Microwave pyrolysis	ACN, 240°C, 10 min	7	3	0	0	45	2	0
		345	9.0	Gas-phase pyrolysis	200°C, 5 min	67	5	3	0	0	0	0
		261	3.1/3.4/4.4	Gas-phase pyrolysis	200°C, 10 min	14	13	0	2	11	0	0
		263	4.3	Photolysis		0	211	0	0	263	0	0
		263	7.5/7.7/10.3	Photolysis		0	211	0	0	263	0	0

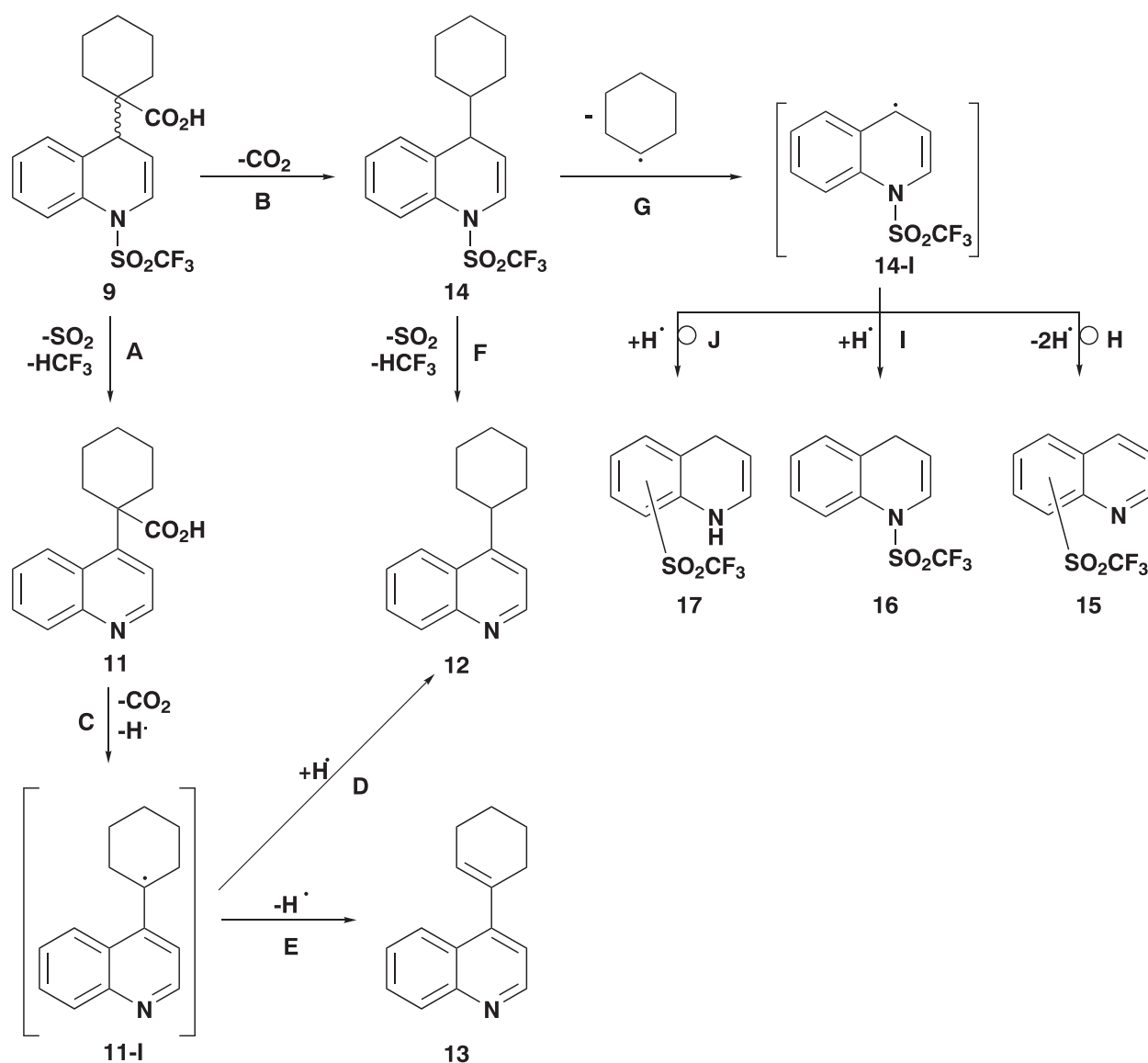
The analysis of all products and reaction conditions resulted in the reaction mechanism proposed for compound **9**, which is presented in Scheme 1. This mechanism is proposed mainly on the basis of thermolyses in gas and solution phases (MIP). The scheme illustrates both competitive processes: the loss of SO_2CF_3 (way A) and the loss of CO_2 (way B). Way A involves the reaction that is of our interest (rearomatization of the pyridine ring allowing a second possible substitution on the ring after a new activation of the nitrogen). Unfortunately, compound **11** proved to be unstable, suffering elimination of CO_2 (way C) under all conditions tested and affording intermediate (**11I**). From this radical, compound **12** would be generated by hydrogen abstraction (way D), while **13** is produced by hydrogen loss (path E).

On the other hand, way B, which is the other competitive process, affords compound **14** (which still possesses

the trifluoromethyl moiety). Nevertheless, it is also unstable and decomposes into compound **12** (through a rearomatization reaction by the loss of SO_2CF_3 , way F) and the intermediate **14I** by the breaking of the C–C bond between the heterocycle and the cyclohexyl moiety (path G). This unstable radical reorganizes to yield a complex mixture of compounds (ways H, I, and J; compounds **15–17**, respectively), which were isolated as a mixture.

2.3 | Reactions of 1-(3-cyano-1-((trifluoromethyl)sulfonyl)-1,4-dihydropyridin-4-yl)cyclohexane-1-carboxylic acid (**10**)

The identification of all products of the reactions of **10** was performed through the analysis of GC/MS and



SCHEME 1 Proposed mechanism for the thermal and photochemical reactions of **9**

NMR spectra. Once more, as in the case of **9**, under all reaction conditions, the desired compound **18** was obtained (Table 2).

Photolysis was again the most unfavorable method with yields of about 2%. Nevertheless, the partially unsaturated compound **20** (formed from **18** after decarboxylation and elimination of a radical hydrogen) was obtained in 44% yield. Another interesting result is the generation of the mixture of 3 trifluoromethyl sulfonyl unsaturated isomers **22a** to **22c** (42%). This fact confirms that both paths involving loss of small moieties ($-\text{SO}_2\text{CF}_3$ and $-\text{CO}_2$) compete, as was proposed for **9**. A clear evidence that this occurs was the detection of the unsaturated compound **21**, which should come from **10** upon loss of CO_2 .

On the other hand, MIP (230°C, 10 min) was a better method than photolysis for **18** in terms of yield (26%). Nevertheless, the reaction that affords **22a** to **22c** is still the main mechanism of reaction. Additionally, gas-phase pyrolysis was also the best method to produce **18** (74% yield) and provided the possibility of preparing other interesting substituted pyridines (**19** and **20**) just by adjusting the reaction time.

As was proposed for **9** and mainly for the reactions initialized by thermic processes, Scheme 2 shows the mechanism of formation of all compounds obtained from **10**. The scheme shows both competitive processes (ways A and B). The desired aromatic compound is obtained directly from way A. Nevertheless, in any case, it was possible to avoid the decomposition to secondary products (**19-22**).

It is important to note that compounds **19** and **20** were not the target products, but they are interesting substituted pyridines, which could be obtained from the

loss of CO_2 (way C). On the other hand, way B would yield the proposed intermediate **21I**. This could afford the unsaturated hydroxyridine **21** (which in turn would increase the amount of **20**) or fragment itself to intermediate **22I** to form the products **22a** to **22c** (which retain the $-\text{SO}_2\text{CF}_3$ moiety).

For a deeper understanding on the mechanisms of reaction of hydroxyridines **9** and **10**, density functional theory calculations (B3LYP/6-31 + G(d,p)) were performed in both gas and solution phases (Table 3). These calculations provided information about the energy required for the different processes that occur in the reactions, particularly in the thermolysis (gas phase pyrolysis and MIP).

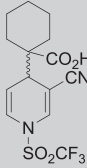
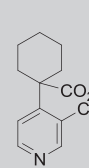
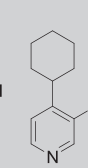
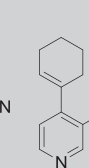
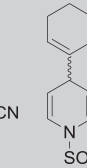
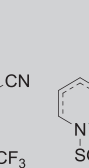
As it is possible to see, the energies required to break the C-C bonds between the cyclohexyl group and the carboxylic acid for both hydroxyridines are higher than the ones required to break the N-S bond (between the hydroxyridine and the trifluoromethyl sulfonyl moiety) or the S-C (between the trifluoromethyl and sulfonyl group), regardless of the phase.

This would perfectly explain why it is always the low-energy path that yields the aromatized compounds (path A, Schemes 1 and 2, and left part of Figure 2, paths A and B) in both cases.

In addition, the energy required to break the S-CF₃ bond (red line, Figure 2) is higher than the one required to break the N-S bond in both cases. These facts allow us to think about the shifting of the SO_2CF_3 moiety as a whole and also justify the fact that many trifluoromethyl sulfonyl isomeric derivatives were obtained.

Other studies performed thermogravimetric analysis and differential thermal analysis (DTA) on **9** and **10** (see

TABLE 2 Pyrolysis (microwave induced and gas phase) vs photolysis reaction of compound **10**

							
Compound		10	18	19	20	21	22a-c
Gas chromatography reaction	Time, min	9.2	8.4	6.6	6.3	4.3	5.5, 7.1 and 8.1
	<i>m/z</i>	364	230	211	209	318	238
Reaction condition							
Photolysis, %	Acetonitrile, 254 nm	1	2	7	44	2	42
Microwave pyrolysis, %	Acetonitrile, 230°C, 10 min	14	26	7	7	1	43
Gas-phase pyrolysis, %	200°C, 5 min	5	74	2	8	0	1
	200°C, 10 min	2	48	20	28	0	1
	200°C, 20 min	0	36	15	26	0	2

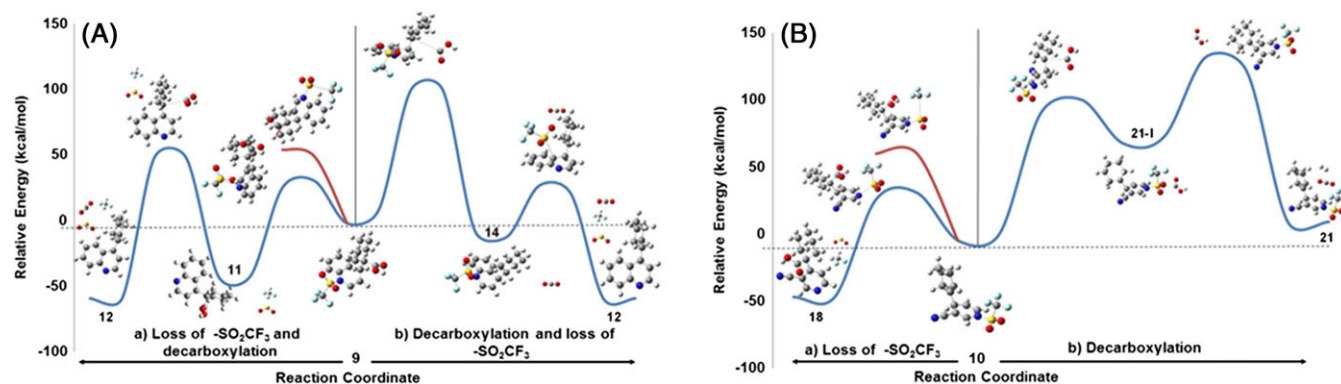


FIGURE 2 Reaction coordinates in the gas phase for different breaking bonds of compounds **9** (A) and **10** (B)

compounds. This conclusion would be reached also from the calculations performed, where all the gas-phase energy barriers calculated for compound **9** are lower than those for compound **10**.

3 | CONCLUSIONS

Through the use of the 3 methodologies used in the present article, it was possible to achieve the desired substituted pyridines. Nevertheless, this work shows one more time the usefulness of the gas-phase pyrolysis, in this particular case to complete the sequence of activation-substitution-deprotection in the generation of heterocycles that are difficult to prepare by other methods. Through experimental observations and quantum chemical calculations, we were able to rationalize the sequence and the energy requirements of the different processes for each compound. Moreover, we found that 2 competitive processes occur in the thermolysis reactions of **9** and **10**. However, the elimination of the CF_3SO_2 moiety for both reactants is the predominant mechanism of reaction. Although the yields are not equally high for both compounds tested, it is particularly important to highlight the purpose of this contribution in the sense of providing a “do it again” method. Nevertheless, further work is still needed to reach a unique and undisputed method.

4 | EXPERIMENTAL SECTION

4.1 | Materials and analytical methods

Pure compounds **9** and **10** were prepared as previously reported^[43] and together with main products were characterized by standard spectroscopic techniques (^1H , ^{13}C , ^{19}F , and UV) and mass spectrometry. All data are in agreement with the proposed structures. Nuclear magnetic resonance spectra were recorded in chloroform-*d*

with a Bruker Avance II 400-MHz spectrometer (BBI probe, *z* gradient) (^1H at 400.16 MHz, ^{13}C at 100.56 MHz, and ^{19}F at 376.53 MHz). Chemical shifts are reported in parts per million downfield from trimethylsilyl. The spectra were measured at 25°C. Absorption spectra were recorded with a UV-1601 Shimadzu spectrophotometer, using a quartz cell with an optical path length of 1 cm. Infrared spectra were recorded with an FT-IR Bruker IFS 28 spectrometer, with a resolution of 2 cm^{-1} in the range from 4000 to 400 cm^{-1} by using KBr disks for solid samples or a quartz cell fitted with KBr windows. Gas chromatography/mass spectrometry analysis was performed with a Shimadzu GC/MS QP 5050 spectrometer equipped with a VF column ($30\text{ m} \times 0.25\text{ mm} \times 5\text{ }\mu\text{m}$) by using helium as an eluent at a flow rate of 1.1 mL min^{-1} . The injector and the ion source temperature was 280°C, and the oven heating ramp was $15^\circ\text{C min}^{-1}$ from 200°C up to 280°C. The pressure in the MS instrument was 10^{-5} Torr, precluding ion-molecule reactions, and MS recordings were made in the electron impact (EI) mode at an ionization energy of 70 eV. High-resolution mass spectra were recorded at the University of Vigo, Spain.

Thermogravimetric measurements were performed using a Shimadzu DTG-60 thermoanalyzer, under an oxidizing atmosphere (air) with a gas flux of 75 mL min^{-1} , a heating rate of $10^\circ\text{C min}^{-1}$, and 30°C to 600°C temperature range.

4.2 | Photolysis reactions

Solutions of compounds **9** and **10** in ACN ($(6 \pm 1) \times 10^{-5}\text{ M}$ and $(22.2 \pm 0.4) \times 10^{-5}\text{ M}$, respectively) were photolyzed by using low-pressure mercury lamps emitting at 254 nm, and their decomposition was followed by UV spectroscopy (see Figures SA and SB, page S14 in the supporting information). Only for compound **10** were we able to obtain the photodegradation rate, measuring the decay at 270 nm ($k_{25} = (3.5 \pm 0.2) \times 10^{-3}\text{ s}^{-1}$). This

was determined from the slope in the linear region of a plot of intensity vs irradiation time. The experiments were performed at different temperatures (25°C, 35°C, 45°C, and 55°C) without change in the rate constant values, which allows us to conclude that this reaction is a purely photochemical process. Preparative photolysis in ACN (100 mL, $(1.0 \pm 0.2) \times 10^{-4}$ M) was performed to identify the photoproducts, and then the reaction mixtures were analyzed by GC/MS spectrometry (Tables 1 and 2).

4.3 | Gas-phase pyrolysis reactions

Static pyrolysis reactions were performed in gas phase (using a vacuum-sealed tube) to compare the products and yields obtained with those provided by photolysis reactions. The goal was to find the method that maximizes the aromatized pyridines.

The static pyrolysis of **9** and **10** was performed by using a tube furnace with a temperature controller device. The substrates (50 mg, 0.128 mmol; 50 mg, 0.137 mmol for **9** and **10**, respectively) were each introduced into a reaction tube (1.5 cm \times 12 cm Pyrex), sealed under vacuum (0.06 mbar) and then placed inside the furnace for 5 to 20 minutes at 200°C. The resultant pale yellow reaction mixtures were then extracted with solvents (ethyl acetate for GC/MS and acetone-*d*₆ for NMR analyses), analyzed through GC/MS, and subjected to purification (preparative plate chromatography in dichloromethane : ethyl acetate [95:5]) (Tables 1 and 2).

4.4 | Microwave-induced pyrolysis

Microwave-induced pyrolysis was performed in a microwave reactor Monowave 300 Anton Paar, using 10-mL microwave tubes. The reaction temperatures were measured by infrared surface detector during the microwave heating. A suspension of either **9** (20 mg, 0.051 mmol) or **10** (20 mg, 0.055 mmol) in ACN was irradiated in the microwave reactor at the temperature and time indicated in each case. After cooling to room temperature, the mixture was analyzed by GC/MS and then subjected to purification (preparative plate chromatography in dichloromethane : ethyl acetate [95:5]) (Tables 1 and 2).

4.5 | Calculations

All calculations were performed with the GAUSSIAN09 program.^[44] The geometric parameters for all the reactants, transition states, and products of the studied reactions were fully optimized using density functional theory (density functional theory and TD-DFT with B3LYP/6-31 + G(d,p)) approaches. This work used computational resources from CCAD, Universidad Nacional

de Córdoba (<http://ccad.unc.edu.ar/>), in particular the Mendieta Cluster, which is part of SNCAD, MinCyT, República Argentina.

4.6 | Characterization

4.6.1 | 1-(1-((Trifluoromethyl)sulfonyl)-1,4-dihydroquinolin-4-yl)cyclohexane-1-carboxylic acid (**9**)

mp: 160°C to 161°C (white amorphous solid). ¹⁹F NMR (376 MHz, CDCl₃): δ (ppm) = -75.11. ¹H NMR (400 MHz, CDCl₃): δ (ppm) = 7.57 (1H, d, J = 8.4 Hz), 7.31 (1H, td, J_1 = 7.92 Hz, J_2 = 1.55 Hz), 7.21 (1H, td, J_1 = 7.54 Hz, J_2 = 1.04 Hz), 7.14 (1H, dd, J_1 = 7.84 Hz, J_2 = 1.50 Hz), 6.77 (1H, d, J = 7.53 Hz), 5.58 (1H, dd, J_1 = 6.40 Hz, J_2 = 8.11 Hz), 5.53 (1H, s broad, OH), 3.66 (1H, d, J = 6.40 Hz), 2.18 (1H, d, J = 12.80 Hz), 2.01 (1H, d, J = 8.29 Hz), 1.64 (3H, m), 1.37 (3H, m), 1.19 (1H, m), 1.06 (1H, m). ¹³C NMR (100 MHz, CDCl₃): δ (ppm) = 179.9, 135.6, 130.8, 127.9, 127.3, 126.9, 126.0, 120.2 (J_{C-F} = 2.36 Hz), 119.8 (J_{C-F} = 323.22 Hz), 113.9, 54.5, 46.4, 30.4 ($\times 2$), 25.5, 23.4, 23.3. IR (KBr, cm⁻¹): 2952.4, 2926.4, 2973.4, 1697.0, 1495.5, 1487.8, 1462.7, 1454.0, 1402.0, 1388.5, 1287.2, 1250.6, 1234.2, 1227.4, 1196.6, 1191.8, 1154.1, 1149.3, 1123.3, 1078.8, 1072.2, 1052.9, 1010.5, 929.5, 753.0, 739.5, 680.7, 611.3, 600.7, 575.6. GC: 11.795 minutes. MS (EI): m/z (%) = 389 (M+, 8), 265 (4), 264 (31), 263 (7), 262 (72), 256 (3), 228 (6), 213 (4), 212 (17), 211 (3), 210 (15), 200 (3), 198 (5), 186 (6), 185 (5), 184 (15), 182 (5), 170 (4), 168 (5), 167 (4), 158 (3), 157 (3), 156 (11), 154 (5), 146 (6), 144 (6), 143 (5), 142 (3), 132 (6), 131 (13), 130 (100), 129 (31), 128 (12), 127 (4), 126 (7), 118 (8), 117 (6), 115 (5), 110 (20), 109 (3), 106 (3), 103 (8), 102 (6), 91 (7), 89 (3), 83 (4), 82 (3), 81 (16), 79 (6), 78 (3), 77 (15), 69 (9), 67 (9), 65 (3), 55 (7), 53 (4), 51 (3), 41 (9).

4.6.2 | 1-(3-Cyano-1-((trifluoromethyl)sulfonyl)-1,4-dihydropyridin-4-yl)cyclohexane-1-carboxylic acid (**10**)

mp: 169°C to 170°C (white amorphous solid). ¹⁹F NMR (376 MHz, CDCl₃): δ (ppm) = -74.72. ¹H NMR (400 MHz, CDCl₃): δ (ppm) = 7.64 (1H, s), 6.82 (1H, d, J = 8.16 Hz), 5.49 (1H, dd, J_1 = 8.23 Hz, J_2 = 5.40 Hz), 3.45 (1H, d, J = 5.25 Hz), 2.87 (1H, s broad, OH), 2.14 (2H, m), 1.66 (3H, m), 1.41 (4H, m), 1.19 (1H, m). ¹³C NMR (100 MHz, CDCl₃): δ (ppm) = 179.8, 136.4, 122.8, 117.6, 109.6, 94.9, 53.7, 42.3, 30.2 ($\times 2$), 25.5, 23.2, 23.1. IR (KBr, cm⁻¹): 2939.9, 2187.7, 1682.5, 1673.9, 1620.8, 1420.3, 1292.0, 1250.6, 1234.2, 1226.5, 1196.6, 1182.1, 1134.9, 1050.0, 670.1, 612.9, 579.5. GC: 9.178 minutes.

MS (EI): m/z (%) = 364 (M+, 6), 232 (5), 231 (37), 175 (7), 160 (10), 123 (12), 110 (9), 109 (100), 107 (3), 106 (24), 105 (4), 92 (3), 82 (3), 81 (37), 80 (4), 79 (14), 78 (30), 77 (5), 69 (12), 67 (5), 65 (3), 54 (3), 53 (6), 51 (9), 41 (7). High-resolution MS (electrospray ionization time of flight): Calcd for $C_{14}H_{15}F_3N_2O_4S$ $[M + Na]^+$ = 387.05 968, found = 387.05 876.

4.6.3 | 1-(Quinolin-4-yl)cyclohexane-1-carboxylic acid (11)

GC: 9.326 minutes. MS (EI): m/z (%) = 256 (2), 255 (M+, 13), 254 (19), 253 (100), 227 (5), 226 (9), 225 (53), 224 (35), 213 (3), 211 (4), 210 (16), 209 (3), 208 (5), 199 (8), 198 (22), 197 (47), 196 (39), 195 (3), 185 (4), 184 (14), 183 (39), 182 (69), 181 (4), 180 (9), 171 (7), 170 (19), 169 (14), 168 (18), 167 (17), 166 (8), 165 (3), 159, 156 (6), 155 (6), 154 (22), 153 (6), 152 (7), 151 (3), 146 (3), 145 (5), 143 (7), 142 (12), 141 (16), 140 (12), 139 (8), 132 (3), 131 (3), 130 (22), 129 (63), 128 (20), 127 (18), 126 (7), 118 (3), 117 (8), 116 (7), 115 (29), 114 (16), 113 (10), 110 (3), 105 (4), 104 (3), 103 (4), 102 (13), 101 (7), 100 (3), 91 (5), 90 (4), 89 (10), 88 (8), 87 (6), 86 (3), 81 (3), 79 (5), 78 (4), 77 (18), 76 (8), 75 (7), 74 (4), 67 (5), 65 (4), 64 (4), 63 (10), 62 (4), 55 (4), 53 (4), 52 (3), 51 (8), 50 (4), 41 (9).

4.6.4 | 4-Cyclohexylquinoline (12)

GC: 6.79 minutes. MS (EI): m/z (%) = 212 (14), 211 (M+, 100), 210 (29), 196 (4), 183 (7), 182 (19), 180 (11), 170 (8), 169 (9), 168 (46), 167 (35), 166 (15), 157 (7), 156 (387), 155 (33), 154 (54), 152 (6), 144 (7), 143 (56), 142 (17), 140 (4), 139 (5), 130 (10), 129 (12), 128 (9), 127 (15), 126 (5), 116 (4), 115 (19), 102 (6), 101 (7), 89 (5), 77 (7), 76 (4), 75 (6), 41 (10).

4.6.5 | 4-(Cyclohex-1-en-1-yl)quinolone (13)

GC: 6.456 minutes. MS (EI): m/z (%) = 210 (12), 209 (M+, 100), 208 (36), 194 (9), 193 (4), 192 (7), 191 (4), 182 (3), 181 (30), 180 (90), 179 (5), 169 (6), 168 (13), 167 (52), 166 (85), 155 (6), 154 (18), 153 (14), 152 (16), 151 (4), 140 (5), 139 (8), 138 (3), 127 (10), 126 (6), 115 (8), 101 (5), 89 (4), 79 (5), 77 (5), 75 (6), 69 (2), 66 (2), 64 (2), 63 (4), 52 (3), 51 (3), 43 (3).

4.6.6 | 4-Cyclohexyl-1-((trifluoromethyl)sulfonyl)-1,4-dihydroquinoline (14)

GC: 8.966 minutes. MS (EI): m/z (%) = 346 (4), 345 (M+, 14), 262 (3), 239 (3), 225 (9), 214 (6), 213 (7), 212 (49), 211 (14), 210 (28), 209 (3), 208 (5), 198 (11), 197 (4), 196 (9),

185 (3), 184 (3), 183 (4), 182 (9), 181 (5), 180 (10), 176 (3), 171 (4), 170 (10), 169 (8), 168 (28), 167 (18), 165 (3), 158 (5), 157 (4), 156 (11), 155 (9), 154 (12), 153 (4), 152 (5), 145 (3), 144 (16), 143 (10), 142 (13), 141 (3), 140 (4), 139 (3), 134 (3), 132 (6), 131 (11), 130 (100), 129 (9), 128 (10), 127 (8), 118 (20), 117 (19), 116 (6), 115 (13), 114 (3), 107 (6), 106 (8), 103 (5), 102 (4), 101 (3), 95 (20), 94 (4), 93 (5), 91 (12), 90 (8), 89 (6), 81 (12), 79 (14), 78 (5), 77 (12), 69 (8), 67 (11), 65 (6), 63 (3), 55 (3), 54 (3), 50 (3), 41 (9).

4.6.7 | ((Trifluoromethyl)sulfonyl)quinoline (15a-c)

- GC: 3.167 minutes. MS (EI): m/z (%) = 262 (2), 261 (M+, 16), 193 (2), 192 (15), 129 (11), 128 (100), 127 (2), 102 (4), 101 (35), 100 (4), 89 (3), 77 (4), 76 (3), 75 (17), 74 (5), 69 (7), 51 (7), 50 (4).
- GC: 3.463 minutes. MS (EI): m/z (%) = 262 (2), 261 (M+, 14), 193 (4), 192 (37), 176 (2), 148 (2), 129 (13), 128 (100), 127 (6), 116 (2), 102 (11), 101 (30), 100 (4), 89 (2), 77 (10), 76 (4), 75 (13), 74 (7), 51 (9), 50 (5).
- GC: 4.685 minutes. MS (EI): m/z (%) = 261 (M+, 14), 194 (3), 193 (5), 192 (56), 176 (3), 129 (12), 128 (100), 127 (7), 116 (4), 102 (9), 101 (35), 100 (5), 89 (3), 77 (12), 76 (5), 75 (17), 74 (8), 69 (10), 63 (4), 62 (3), 52 (3), 51 (8), 50 (5).

4.6.8 | 1-((Trifluoromethyl)sulfonyl)-1,4-dihydroquinoline (16)

GC: 4.342 minutes. MS (EI): m/z (%) = 264 (2), 263 (M+, 6), 262 (38), 236 (4), 198 (6), 178 (5), 169 (5), 147 (4), 142 (9), 140 (4), 130 (9), 129 (100), 128 (15), 116 (5), 115 (5), 103 (5), 102 (15), 101 (6), 89 (6), 77 (5), 76 (7), 75 (4), 73 (7), 69 (12), 67 (3), 63 (4), 52 (3), 51 (7), 50 (3), 43 (3).

4.6.9 | 8-((Trifluoromethyl)sulfonyl)-1,4-dihydroquinoline (17a-c)

- GC: 7.552 minutes. MS (EI): m/z (%) = 264 (5), 263 (M+, 10), 262 (96), 214 (11), 213 (3), 198 (9), 185 (5), 178 (3), 130 (15), 129 (100), 128 (11), 103 (4), 102 (12), 81 (15), 79 (6), 77 (4), 76 (3), 69 (5), 67 (4), 53 (3), 51 (5), 41 (4).
- GC: 7.727 minutes. MS (EI): m/z (%) = 264 (7), 263 (M+, 10), 262 (89), 235 (6), 209 (14), 208 (4), 198 (14), 194 (5), 181 (4), 180 (20), 178 (7), 168 (3), 167 (4), 166 (4), 156 (3), 152 (4), 148 (3), 143 (5), 142 (4), 135 (3), 130 (24), 129 (100), 128 (11), 127 (3), 115 (5), 103 (5), 102 (17), 99 (3), 81 (10), 79 (6), 77 (5), 76 (5), 73 (4), 69 (5), 67 (4), 53 (4), 51 (4), 41 (4).

c. GC: 10.262 minutes. MS (EI): m/z (%) = 263 (M+, 8), 262 (59), 261 (2), 207 (5), 198 (5), 178 (4), 130 (19), 129 (100), 128 (18), 103 (5), 102 (16), 101 (5), 81 (5), 78 (3), 77 (4), 76 (8), 75 (4), 74 (4), 73 (5), 69 (4), 65 (3), 64 (4), 63 (3), 55 (3), 54 (3), 53 (3), 51 (6), 50 (4), 41 (4).

4.6.10 | 1-(3-Cyanopyridin-4-yl)cyclohexane-1-carboxylic acid (18)

^1H NMR (400 MHz, dimethyl sulfoxide- d_6): δ (ppm) = 11.51 (1H, s), 9.22 (1H, s), 8.92 (1H, d, J = 5.65 Hz), 8.06 (1H, d, J = 5.78 Hz), 5.60 (1H, s broad, OH), 1.94 (5H, m), 1.74 (1H, m), 1.62 (2H, m), 1.44 (1H, m), 1.27 (1H, m). ^{13}C NMR (100 MHz, dimethyl sulfoxide- d_6): δ (ppm) = 175.0, 162.7, 158.2, 150.7, 146.6, 122.2, 121.8, 45.9, 35.1 ($\times 2$), 24.0, 21.4 ($\times 2$). GC: 8.390 minutes. MS (EI): m/z (%) = 231 (3), 230 (M+, 20), 176 (10), 175 (100), 162 (8), 158 (5), 157 (22), 131 (3), 130 (5), 129 (14), 103 (3), 102 (4), 89 (3), 78 (4), 77 (5), 76 (4), 75 (3), 65 (3), 63 (3), 51 (5), 50 (3), 41 (4). High-resolution MS (electrospray ionization time of flight): Calcd for $\text{C}_{13}\text{H}_{14}\text{N}_2\text{O}_2$ [M + H]⁺ = 231.11 280, found = 231.11 241.

4.6.11 | 4-Cyclohexylnicotinonitrile (19)

GC: 3.697 minutes. MS (EI): m/z (%) = 187 (12), 186 (M+, 49), 185 (28), 172 (3), 71 (8), 170 (3), 169 (9), 168 (23), 167 (4), 159 (7), 158 (38), 157 (73), 156 (4), 155 (4), 154 (3), 146 (9), 145 (51), 144 (18), 143 (12), 142 (11), 133 (9), 132 (51), 131 (100), 130 (27), 129 (12), 128 (3), 119 (5), 118 (18), 117 (11), 116 (10), 115 (4), 105 (6), 104 (10), 103 (12), 102 (5), 91 (5), 90 (9), 89 (10), 88 (3), 79 (6), 78 (7), 77 (13), 76 (16), 75 (7), 69 (4), 67 (9), 65 (5), 64 (3), 63 (11), 62 (3), 56 (19), 55 (10), 54 (5), 53 (6), 52 (7), 51 (12), 50 (6), 42 (4), 41 (49).

4.6.12 | 4-(Cyclohex-1-en-1-yl)nicotinonitrile (20)

GC: 3.898 minutes. MS (EI): m/z (%) = 185 (13), 184 (M+, 48), 183 (100), 182 (6), 171 (3), 170 (3), 169 (34), 168 (26), 167 (36), 166 (22), 158 (13), 157 (35), 156 (15), 155 (44), 145 (19), 144 (11), 143 (10), 142 (18), 141 (4), 140 (3), 132 (17), 131 (46), 130 (16), 129 (19), 128 (12), 127 (6), 126 (3), 118 (11), 117 (5), 116 (14), 115 (6), 114 (7), 106 (7), 105 (4), 104 (9), 103 (7), 102 (6), 101 (6), 100 (4), 91 (4), 90 (8), 89 (7), 88 (5), 87 (4), 81 (4), 79 (8), 78 (8), 77 (23), 76 (16), 75 (9), 67 (5), 65 (6), 64 (13), 63 (12), 58 (3), 56 (5), 55 (4), 54 (13), 53 (6), 52 (11), 51 (15), 50 (11), 48 (3), 44 (7), 43 (7), 41 (32).

4.6.13 | 4-(Cyclohex-1-en-1-yl)-1-((trifluoromethyl)sulfonyl)-1,4-dihydropyridine-3-carbonitrile (21)

GC: 4.338 minutes. MS (EI): m/z (%) = 319 (3), 318 (M+, 18), 250 (5), 239 (5), 238 (8), 237 (77), 186 (5), 185 (85), 174 (5), 173 (60), 168 (69), 158 (4), 153 (5), 141 (4), 133 (12), 114 (4), 111 (5), 105 (4), 83 (19), 81 (27), 80 (9), 79 (39), 77 (8), 73 (5), 70 (3), 69 (100), 66 (8), 65 (5), 55 (23), 53 (28), 52 (4), 51 (5), 43 (3), 41 (12).

4.6.14 | 1-((Trifluoromethyl)sulfonyl)-1,2-dihydropyridine-3-carbonitrile (22a)

GC: 5.563 minutes. MS (EI): m/z (%) = 239 (4), 238 (M+, 7), 237 (100), 174 (3), 173 (41), 153 (3), 133 (9), 110 (4), 105 (4), 104 (10), 81 (12), 79 (4), 77 (7), 69 (56), 67 (4), 53 (4), 51 (4), 41 (7).

4.6.15 | 1-((Trifluoromethyl)sulfonyl)-1,4-dihydropyridine-3-carbonitrile (22b)

GC: 7.130 minutes. MS (EI): m/z (%) = 239 (3), 238 (M+, 6), 237 (100), 231 (3), 127 (15), 186 (19), 185 (11), 184 (4), 176 (19), 173 (26), 171 (4), 170 (5), 169 (16), 168 (29), 167 (6), 159 (10), 158 (19), 156 (4), 154 (3), 148 (6), 147 (4), 146 (18), 145 (6), 144 (3), 143 (5), 142 (3), 133 (10), 132 (5), 131 (5), 130 (19), 128 (3), 119 (3), 118 (4), 117 (7), 116 (4), 115 (3), 109 (4), 105 (5), 104 (6), 103 (5), 102 (4), 91 (5), 90 (4), 89 (6), 81 (15), 79 (7), 78 (6), 77 (12), 76 (6), 75 (3), 69 (28), 67 (7), 65 (6), 63 (6), 55 (4), 54 (5), 53 (6), 52 (3), 51 (8), 50 (5), 41 (10).

4.6.16 | 1-((Trifluoromethyl)sulfonyl)-1,6-dihydropyridine-3-carbonitrile (22c)

GC: 8.080 minutes. MS (EI): m/z (%) = 239 (5), 238 (M+, 9), 237 (100), 174 (4), 173 (43), 153 (3), 133 (10), 109 (3), 105 (6), 104 (9), 81 (12), 79 (5), 78 (3), 77 (7), 69 (57), 67 (4), 55 (4), 53 (5), 50 (3), 43 (4), 41 (8).

ACKNOWLEDGEMENTS

Thanks are due for the financial support provided by MINCYT-CONACYT (MX/12/07), CONICET, CONACyT 191400 FOINS, FONCyT, MINCYT, and SECyT-UNC. This work used computational resources from CCAD, Universidad Nacional de Córdoba (<http://ccad.unc.edu.ar/>), in particular the Mendieta Cluster, which is part of SNCAD, MinCyT, República Argentina. G.F. and M.V.C. thank CONICET for their doctoral fellowships.

ORCID

Walter J. Peláez  <http://orcid.org/0000-0001-6950-5312>

REFERENCES

- [1] M. V. Cooke, I. Malvacio, W. J. Peláez, A. J. Pepino, M. R. Mazzieri, G. A. Argüello, *RSC Adv.* **2015**, 5(33), 26255, <https://doi.org/10.1039/C5RA00249D>.
- [2] W. J. Peláez, T. M. V. D. Pinho e Melo, *Tetrahedron* **2013**, 69(18), 3646, <https://doi.org/10.1016/j.tet.2013.03.017>.
- [3] W. J. Peláez, A. J. Pepino, G. A. Argüello, T. M. V. D. Pinho e Melo, *Eur. J. Org. Chem* **2014**, 2014(14), 2933, <https://doi.org/10.1002/ejoc.201301922>.
- [4] J. W. Daly, H. M. Garraffo, T. F. Spande, in *Alkaloids: Chemical and Biological Perspectives*, (Ed: S. W. Pelletier), Elsevier, New York **1999**.
- [5] A. J. Boulton, A. McKillop, in *Comprehensive Heterocyclic Chemistry*, (Eds: A. R. Katritzky, W. R. Charles), Pergamon, Oxford **1984**.
- [6] J. B. Harper, in *Comprehensive Heterocyclic Chemistry III*, (Eds: A. R. Katritzky, A. R. Christopher, F. V. S. Eric, J. K. T. Richard), Elsevier, Oxford **2008**.
- [7] J. Bosch, M. L. Bennasar, *Synlett* **1995**, 6, 587.
- [8] A. Sinclair, R. A. Stockman, *Nat. Prod. Rep.* **2007**, 24(2), 298, <https://doi.org/10.1039/b604203c>.
- [9] M. F. Gordeev, D. V. Patel, B. P. England, S. Jonnalagadda, J. D. Combs, E. M. Gordon, *Biorg. Med. Chem.* **1998**, 6(7), 883, [https://doi.org/10.1016/S0968-0896\(98\)00048-0](https://doi.org/10.1016/S0968-0896(98)00048-0).
- [10] V. A. Burgess, S. G. Davies, R. T. Skerlj, *Tetrahedron: Asymmetry* **1991**, 2(5), 299, [https://doi.org/10.1016/S0957-4166\(00\)82109-6](https://doi.org/10.1016/S0957-4166(00)82109-6).
- [11] S. Goldmann, J. Stoltefuss, *Angew. Chem. Int. Ed. Engl.* **1991**, 30(12), 1559, <https://doi.org/10.1002/anie.199115591>.
- [12] M. G. P. Buffat, *Tetrahedron* **2004**, 60(8), 1701, <https://doi.org/10.1016/j.tet.2003.11.043>.
- [13] F. X. Felpin, J. Lebreton, *Eur. J. Org. Chem.* **2003**, 19, 3693.
- [14] J. S. Carey, D. Laffan, C. Thomson, M. T. Williams, *Org. Biomol. Chem.* **2006**, 4(12), 2337, <https://doi.org/10.1039/b602413k>.
- [15] R. W. Dugger, J. A. Ragan, D. H. B. Ripin, *Org. Process Res. Dev.* **2005**, 9(3), 253, <https://doi.org/10.1021/op050021j>.
- [16] D. M. Stout, A. I. Meyers, *Chem. Rev.* **1982**, 82(2), 223, <https://doi.org/10.1021/cr00048a004>.
- [17] R. Kumar, R. Chandra, R. in *Advances in Heterocyclic Chemistry*, (Ed: A. R. Katritzky), Academic Press **2001** 269.
- [18] A. Sausins, G. Duburs, *Heterocycles* **1988**, 27, 291.
- [19] J. P. Kutney, *Heterocycles* **1977**, 7(1), 593, <https://doi.org/10.3987/S-1977-01-0593>.
- [20] D. L. Comins, S. O'Connor, in *Advances in Heterocyclic Chemistry*, (Ed: A. R. Katritzky), Academic Press **1988** 199.
- [21] T. Itoh, H. Hasegawa, K. Nagata, Y. Matsuya, M. Okada, A. Ohsawa, *Chem. Pharm. Bull.* **1994**, 42(9), 1768, <https://doi.org/10.1248/cpb.42.1768>.
- [22] M. Wada, Y. Nishihara, K. Y. Akiba, *Tetrahedron Lett.* **1985**, 26(27), 3267, [https://doi.org/10.1016/S0040-4039\(00\)98168-1](https://doi.org/10.1016/S0040-4039(00)98168-1).
- [23] J. A. Bull, J. J. Mousseau, G. Pelletier, A. B. Charette, *Chem. Rev.* **2012**, 112(5), 2642, <https://doi.org/10.1021/cr200251d>.
- [24] D. L. Comins, Y. C. Myoung, *J. Org. Chem.* **1990**, 55(1), 292, <https://doi.org/10.1021/jo00288a049>.
- [25] Z. Sun, S. Yu, Z. Ding, D. Ma, *J. Am. Chem. Soc.* **2007**, 129(30), 9300, <https://doi.org/10.1021/ja0734849>.
- [26] T. Itoh, M. Miyazaki, K. Nagata, A. Ohsawa, *Heterocycles* **1997**, 46, 83.
- [27] A. B. Charette, M. Grenon, A. Lemire, M. Pourashraf, J. Martel, *J. Am. Chem. Soc.* **2001**, 123(123), 11829, <https://doi.org/10.1021/ja017136x>.
- [28] S. Raussou, R. Gosmini, P. Mangeney, A. Alexakis, M. Commerçon, *Tetrahedron Lett.* **1994**, 35(30), 5433, [https://doi.org/10.1016/S0040-4039\(00\)73518-0](https://doi.org/10.1016/S0040-4039(00)73518-0).
- [29] R. A. Toscano, M. D. C. Hernandez Galindo, R. Rosas, O. Garcia Mellado, F. del Rio Portilla, C. Amabile Cuevas, C. Alvarez Toledano, *Chem. Pharm. Bull.* **1997**, 45(6), 957, <https://doi.org/10.1248/cpb.45.957>.
- [30] R. A. Toscano, R. Rosas, M. D. C. Hernandez Galindo, C. Alvarez Toledano, O. Garcia Mellado, *Transition Met. Chem.* **1998**, 23(2), 113, <https://doi.org/10.1023/A:1006978622592>.
- [31] A. R. Katritzky, S. Zhang, T. Kurz, M. Wang, P. Steel, *J. Org. Lett.* **2001**, 3(18), 2807, <https://doi.org/10.1021/ol101116f>.
- [32] D. L. Comins, S. P. Joseph, in *Advances in Nitrogen Heterocycles* (Edited by C. J. Moody), Greenwich, CT **1996**, ch. 6.
- [33] H. Rudler, B. Denise, A. Parlier, J. C. Daran, *Chem. Commun.* **2002**, (9), 940, <https://doi.org/10.1039/b201780f>.
- [34] E. Ullah, S. Rotzoll, A. Schmidt, D. Michalik, P. Langer, *Tetrahedron Lett.* **2005**, 46(52), 8997, <https://doi.org/10.1016/j.tetlet.2005.10.108>.
- [35] A. Schmidt, D. Michalik, S. Rotzoll, E. Ullah, C. Fischer, H. Reinke, H. Gols, P. Langer, *Org. Biomol. Chem.* **2008**, 6(15), 2804, <https://doi.org/10.1039/b804139c>.
- [36] N. Gualo Soberanes, M. C. Ortega Alfaro, J. G. Lopez Cortés, R. A. Toscano, H. Rudler, C. Alvarez Toledano, *Tetrahedron Lett.* **2010**, 51(24), 3186, <https://doi.org/10.1016/j.tetlet.2010.04.030>.
- [37] A. Garduño Alva, Y. Xu, N. Gualo Soberanes, J. Lopez Cortés, H. Rudler, A. Parlier, M. C. Ortega Alfaro, C. Alvarez Toledano, R. A. Toscano, *Eur. J. Org. Chem.* **2008**, 21, 3714.
- [38] A. Garduño Alva, M. C. Ortega Alfaro, J. G. Lopez Cortés, I. Chávez, J. Barroso Flores, R. A. Toscano, H. Rudler, C. Alvarez Toledano, *Can. J. Chem.* **2012**, 90(5), 469, <https://doi.org/10.1139/v2012-016>.
- [39] P. J. Stang, G. Maas, D. L. Smith, J. A. McCloskey, *J. Am. Chem. Soc.* **1981**, 103(16), 4837, <https://doi.org/10.1021/ja00406a028>.
- [40] C. C. Cheng, *Prog. Med. Chem.* **1969**, 6, 61.

- [41] C. C. Cheng, B. Roth, *Prog. Med. Chem.* **1970**, 7, 285, [https://doi.org/10.1016/S0079-6468\(08\)70356-4](https://doi.org/10.1016/S0079-6468(08)70356-4).
- [42] G. Maas, P. J. Stang, *J. Org. Chem.* **1981**, 46(8), 1606, <https://doi.org/10.1021/jo00321a015>.
- [43] A. Rivera Hernández, G. M. Chans, H. Rudler, J. G. López Cortés, R. A. Toscano, C. Alvarez Toledano, *Tetrahedron* **2014**, 70(10), 1861, <https://doi.org/10.1016/j.tet.2014.01.044>.
- [44] M. J. Frisch, G. W. Trucks, H. B. Schlegel, G. E. Scuseria, M. A. Robb, J. R. Cheeseman, G. Scalmani, V. Barone, B. Mennucci, G. A. Petersson, *Gaussian 09, Revision E.01*, Gaussian, Inc., Wallingford, CT **2009**.

SUPPORTING INFORMATION

Additional Supporting Information may be found online in the supporting information tab for this article.

How to cite this article: Firpo G, Cooke MV, Peláez WJ, et al. Rearomatization of trifluoromethyl sulfonyl dihydropyridines: Thermolysis vs. photolysis. *J Phys Org Chem.* 2017;e3789. <https://doi.org/10.1002/poc.3789>